Supplemental Material for Ultrafast Raman thermometry in driven $YBa_2Cu_3O_{6.48}$

T.-H. Chou[1], M. Först[1], M. Fechner[1], M. Henstridge[1,2], S. Roy[1], M. Buzzi[1], D. Nicoletti[1], Y. Liu[3], S. Nakata[3], B. Keimer[3], A. Cavalleri[1,4]

[1] Max Planck Institute for the Structure and Dynamics of Matter, 22761 Hamburg, Germany

[2] SLAC National Accelerator Laboratory, Menlo Park, 94025 California, USA

[3] Max Planck Institute for Solid State Research, 70569 Stuttgart, Germany

[4] Department of Physics, Clarendon Laboratory, University of Oxford, Oxford OX1 3PU, United Kingdom

S1. Experimental setup

S2. Data processing and analysis

S3. Extrapolating zero-fluence phonon temperatures

S4. Fit and deconvolution of the lattice temperature

S5. Heating calculation

S1. Experimental setup

A Ti:sapphire amplifier system delivering 100-fs pulses at 800 nm wavelength and 1 kHz repetition rate was used to drive an optical parametric amplifier (OPA). The signal and idler outputs were directed into a 1-mm thick GaSe crystal to generate mid-IR pump pulses via difference frequency generation (DFG). The resulting spectrum, measured via Fourier transform infrared spectroscopy and shown in Figure S1b, was centered at 20 THz with an 8-THz FWHM bandwidth to encompass the two infrared-active c-axis polarized apical oxygen phonons of $YBa_2Cu_3O_{6.48}$ at 17.5 and 20 THz. The pump beam was focused onto the sample by a KBr lens, resulting in an excitation fluence of 8 mJ/cm^2. The time-resolved terahertz spectroscopy data shown in the main text (Fig. 1a, 1b, 2b, 2c, 4a, and 4b, taken from Ref. [1]) were measured under the same excitation conditions.

For the Raman scattering experiment, 405-nm probe pulses were generated by second harmonic generation (SHG) from the 800-nm fundamental pulses in a 5-mm thick BBO crystal. The spectrum was cleaned up by a 405-nm bandpass and a home-built grating-based spectral filter. In this way, the bandwidth was reduced to 100 cm^{-1} FWHM.

A cross-correlation measurement between the mid-IR pump and 405-nm probe pulses, using sum-frequency generation in a 10-µm thin $LiNbO_3$ substrate, yielded a time resolution for the experiment of 1.1 ps FWHM, see Figure S1c.

Both pump and probe pulses were polarized along the c-axis of an ac-oriented surface of a $YBa_2Cu_3O_{6.48}$ single crystal. The probe photons scattered from the sample were collected by a pair of aspherical lenses, filtered by a c-axis oriented polarizer and detected by a 500-mm focal length spectrometer equipped with a thermoelectric-cooled CCD detector. A 405-nm notch filter was used to block the strong elastic scattering.

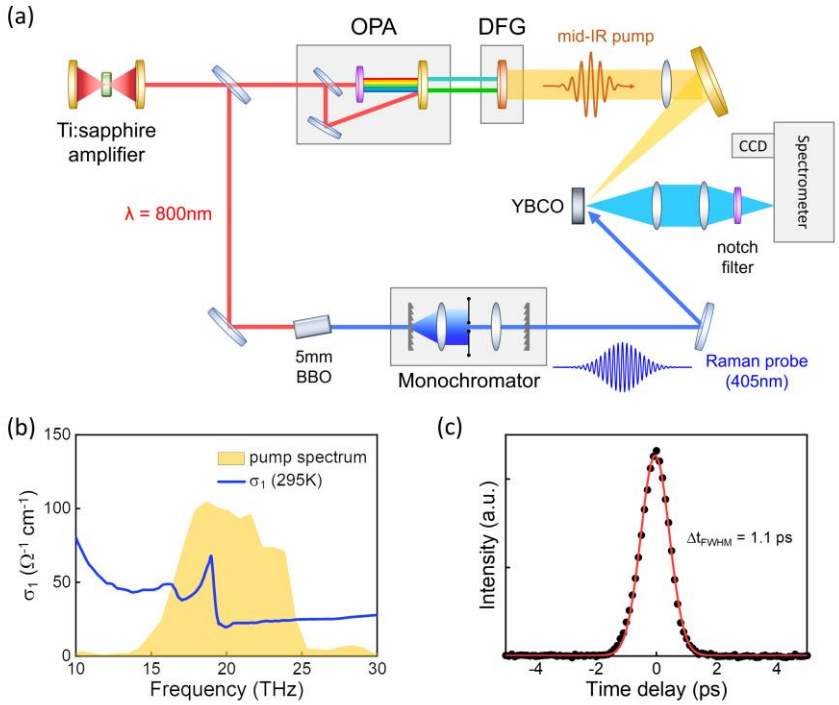

Figure S1: (a) Schematic of the time-resolved spontaneous Raman setup. (b) The yellow filling shows the mid-IR pump spectrum measured by Fourier-transform infrared spectroscopy (FTIR). The blue line is the real part of equilibrium optical conductivity, σ_1, of $YBa_2Cu_3O_{6.48}$ at 295 K. (c) Cross-correlation between the mid-IR pump and 405-nm probe pulses, measured via sum-frequency mixing in a thin $LiNbO_3$ substrate. The extracted time resolution is 1.1 ps FWHM.

S2. Data processing and analysis

The Raman spectra presented in this paper were acquired in the $y(zz)\bar{y}$ geometry. Two polarizers, placed before and after the sample, were aligned along the c-axis of the $YBa_2Cu_3O_{6.48}$ single crystal. Figure S2a shows the raw Raman spectrum taken at a time delay of -5 ps (red curve), together with a background spectrum obtained in the $y(xz)\bar{y}$ geometry. The gray area illustrates the bandwidth of the notch filter used to block the elastic line.

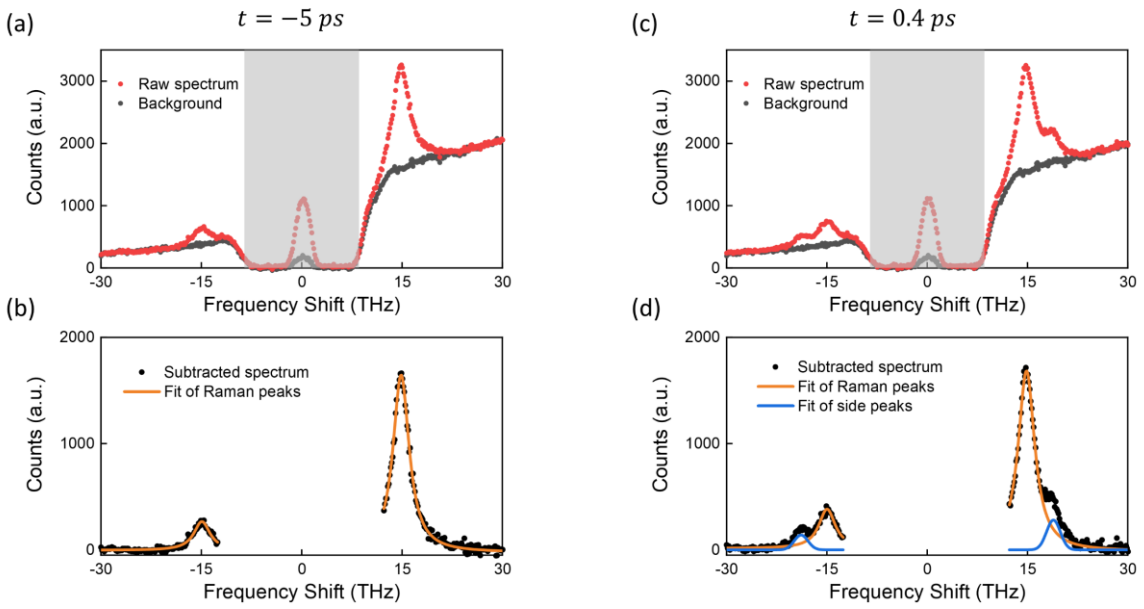

Figure S2: (a) Raw Raman spectrum measured in $YBa_2Cu_3O_{6.48}$ at room temperature and negative time delay (red dots). The black dots show the background spectrum (see text). The gray area indicates the blocking range of the 405-nm notch filter. (b) Background-subtracted Raman spectrum (black), along with a Lorentzian fit to the Stokes and Anti-Stokes peaks at ± 15 THz (orange). (c, d) Same quantities as in (a, b), respectively, measured at a positive time delay t = 0.4 ps. The blue line in (d) is a Gaussian fit to the two peaks at ± 20 THz, which result from nonlinear optical mixing between the pump and the probe pulses within their cross-correlation width.

The Raman spectrum used for the data analysis was achieved by subtracting the background from the raw spectrum (both shown in Fig. S2a) and clearly shows the Stokes and Anti-Stokes peaks of the A_g Raman mode at ± 15 THz (see Fig. S2b, black). This background-subtracted spectrum was fitted by two Lorentzian peaks with equal linewidths to determine the AS/S amplitude ratio.

Figures S2c and S2d show the transient room temperature Raman spectrum measured at a time delay of +0.4 ps. Besides the AS peak enhancement, two additional peaks appear at ± 20 THz frequency. The transient spectra were analyzed by again fitting a Lorentzian function to the Raman peaks (Fig. S2d, orange) and a Gaussian function to the additional peaks (Fig. S2d, blue). The amplitude ratio of the Raman AS and S peaks was extracted from the fitted Lorentzian functions.

We note that the side peaks were observed only when pump and probe pulses were overlapped in time, and their center frequencies match exactly the frequency of the pump pulses. Tuning the mid-IR pump pulses to a frequency of 28 THz made these peaks shift accordingly, suggesting that they originate from a nonlinear optical polarization induced by the electric fields of the visible probe and mid-IR pump pulses. Hence, the Raman spectra in Fig. 3b of the main text are plotted after subtracting both, the background spectrum and these two side peaks.

S3. Extrapolating zero-fluence phonon temperatures

Figure S3 shows the probe fluence dependent AS/S peak intensity ratios on $YBa_2Cu_3O_{6.48}$ in the absence of the mid-IR excitation pulses. At both base temperatures of 295 and 100 K, the AS/S intensity ratio increases linearly with probe fluence. The extrapolated 'zero-fluence' AS/S ratios, obtained by a linear fit to the data, correspond to phonon temperatures that match the base temperatures set by the cryostat.

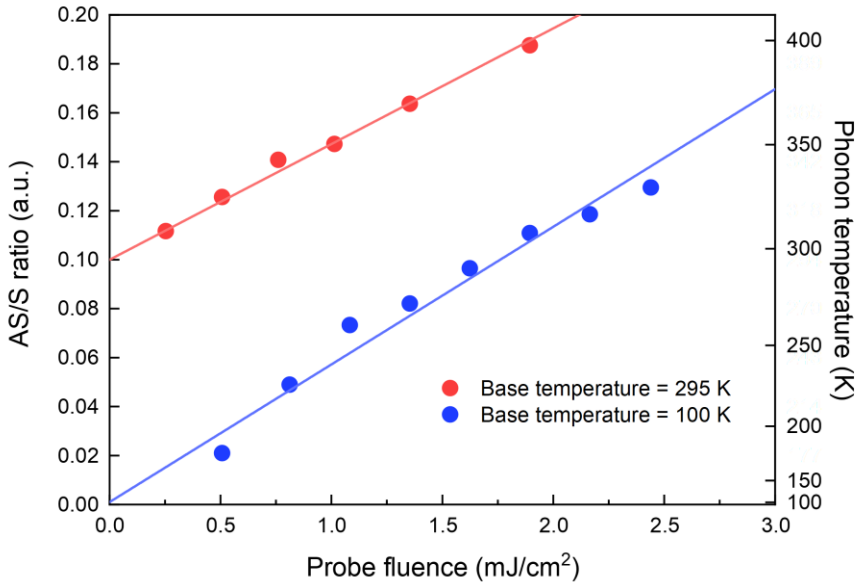

Figure S3: The measured AS/S ratios of the detected 15 THz Raman phonon as a function of the 405-nm probe fluence, for base temperatures of 295 K (red) and 100 K (blue). The phonon temperatures shown on the right axis are calculated from the AS/S ratio on the left axis using Equation 1 of the main text.

This effect was taken into account for the time-resolved experiments, by conducting them at three probe fluences ranging from 0.8 to about 2.0 mJ/cm^2. Figure S4 presents the AS/S peak intensity ratios as a function of time delay under these experimental conditions, for both the nominal base temperatures of 295 and 100 K. To determine the zero-fluence phonon temperature for each time delay, we applied the following procedure. First, we considered all the fluence dependent data at negative delays acquired before the pump reaches the sample (-5 to -0.8 ps) and conducted a linear fit on this combined dataset, similar to what shown in

Figure S3. From this procedure, we extracted the slope of the probe fluence-dependent AS/S peak intensity ratios, constraining the intercept to either 0.1 or 0.001 for 295 or 100 K phonon temperatures, respectively. Subsequently, we fitted the fluence dependent data at each time delay, using the slope obtained from the negative time delay fit, and extracted the zero-fluence AS/S intensity ratios by extrapolating these fits to zero. These values were then converted to the time delay-dependent phonon temperatures. The result of this procedure is shown in Figure 3c of the main text.

The error bars on the phonon temperatures were determined based on the standard errors of the extrapolated zero-fluence AS/S intensity ratios. We then propagated these errors to the extracted phonon temperatures. Note that for the 100 K data, we removed three data points at time delays -1.4, -0.8, and -0.5 ps, where the AS/S ratios were smaller than zero. Additionally, if the AS/S ratios minus one standard error resulted in negative values, the lower bounds of the error bars were set to 0 K.

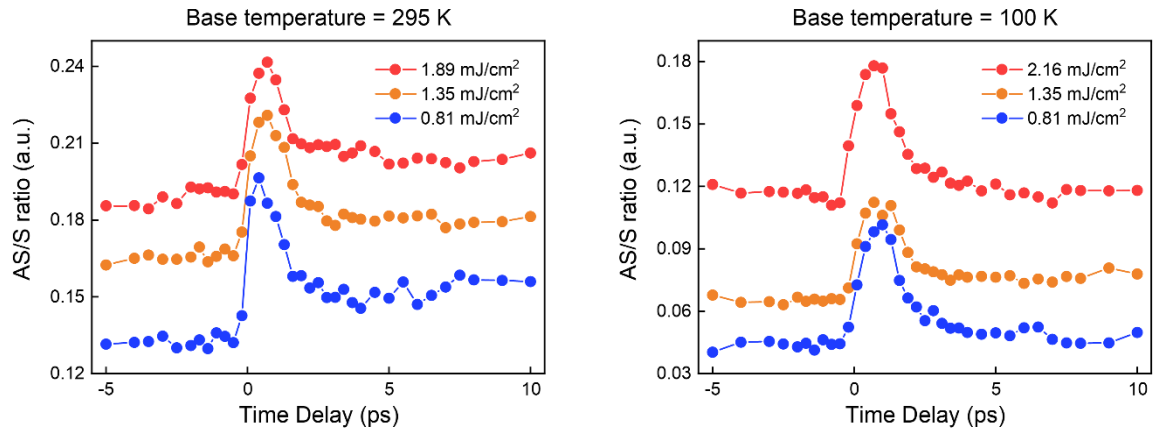

Figure S4: Left panel: Time evolution of the AS/S ratios measured at the base temperature of 295 K with probe fluences of 1.89, 1.35, 0.81 mJ/cm^2. Right panel: Time evolution of AS/S ratios measured at the base temperature of 100 K with probe fluences of 2.16, 1.35, 0.81 mJ/cm^2.

S4. Fit and deconvolution of the lattice temperature

The dynamics of lattice temperature extracted from the time-resolved Raman scattering experiment (see Fig. 3b of the main text) reveal a fast initial heating and an exponential decay to a quasi-equilibrium temperature within a few picoseconds. This behavior can be expressed by the function

$$T(t) = T_0 + \frac{1}{2}A\left(1 + \mathrm{erf}\left(\frac{t}{\sigma}\right)\right)\left[\exp\left(-\frac{t}{\tau_1}\right) + (1 - A_1)\exp\left(-\frac{t}{\tau_2}\right)\right]. \qquad \text{(S1)}$$

Here, T_0 is the base temperature, which is set to either 300 K or 180 K depending on the experimental setting, A is proportional to the initial temperature rise, and $\mathrm{erf}\left(\frac{-t}{\sigma}\right)$ is the error function with σ the time resolution of the experiment. The few-picosecond recovery of the temperature to a quasi-equilibrium value above the base temperature T_0 is described by a double exponential decay with a fast time constant τ_1 and a very long time constant τ_2. The fit results are shown as brown lines in Figure S5.

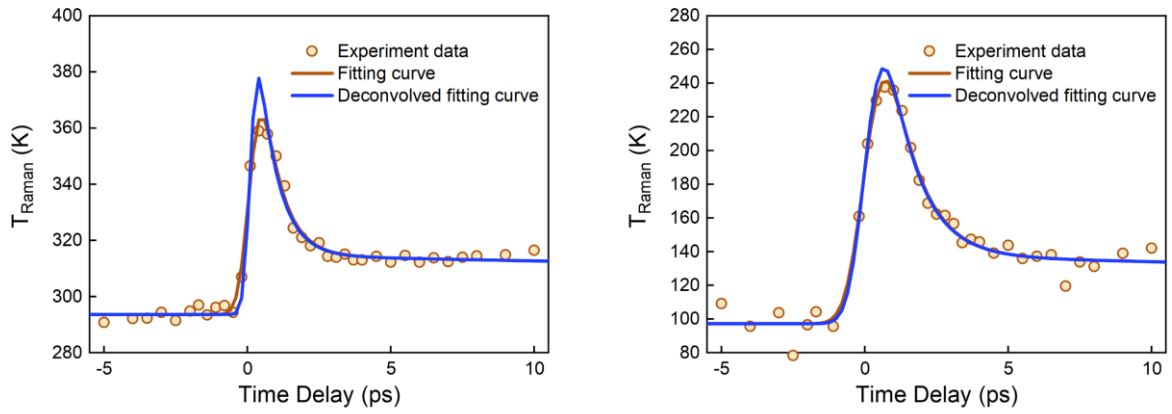

Figure S5: Time evolution of Raman phonon temperature in driven $YBa_2Cu_3O_{6.48}$ measured for 295 (left) and 100 K (right) base temperature. The brown lines are fitting curves to the data, while the blue lines show the deconvolved response obtained after the process described in the text.

The experimentally extracted lattice temperature, as well as the corresponding fits shown above, could potentially be underestimated due to the limited time resolution of the

experiment given. Therefore, we deconvolved the lattice temperature data from the duration of the probe pulse using

$$T_D(t) = iFT\left(\frac{FT(T(t))}{FT(g(t))}\right). \qquad \text{(S2)}$$

Here, $T_D(t)$ is the deconvolved temperature dynamics, FT and iFT represent Fourier transform and inverse Fourier transform, respectively. Furthermore, $T(t)$ is the fitting function introduced in Eq. (S1) and $g(t)$ is the Gaussian envelope function $\frac{1}{c\sqrt{2\pi}}\exp\left(\frac{-t^2}{2c^2}\right)$ where c corresponds to the 600-fs duration (FWHM) of the visible probe pulse.

Figure S5 shows the deconvolved temperature dynamics for the two experimental settings (blue lines). At the base temperature of 295 K, the deconvolved peak lattice temperature is 375 K, equivalent to a temperature rise of 80 K. At the base temperature of 100 K, the peak temperature is 250 K corresponding to a temperature increase of 150 K.

S5. Heating calculation

This section presents the calculations used to estimate the final thermalized temperature at the $YBa_2Cu_3O_{6.48}$ surface after the mid-infrared excitation. The calculation takes into account the total energy absorbed by the sample, the excited volume, and the heat capacity. Following thermalization, but neglecting thermal diffusion, we expect the final temperature to be described by:

$$\rho C_p(T)\frac{\partial T(x,t)}{\partial t} = \frac{1}{d}(1-R)I(t)e^{-x/d} \qquad \text{(S3)}$$

where ρ is the density, $C_p(T)$ is the temperature-dependent heat capacity [2, 3], d is the penetration depth of the pump pulse (which scales from 1.5 – 4 μm), R is the reflectivity, $I(t)$ is the time evolution of the 800-fs Gaussian pump pulse, and x is the space coordinate with x = 0 being the sample surface. For any given initial temperature T_i, we integrated Eq. (S3) in time t to obtain the final temperature distribution $T_f(x,t)$. Since the 50-nm penetration depth of the 405-nm probe is much shorter than that of the mid-IR pump, we report in Fig. 3c of the main text $T_f(0,t)$ as a function of time t for comparison with the experimental data. The measured lattice temperature at long positive time delay agrees with our calculation.

Reference

[1] A. Ribak, M. Buzzi, D. Nicoletti, R. Singla, Y. Liu, S. Nakata, B. Keimer and A. Cavalleri, *Two-fluid dynamics in driven $YBa_2Cu_3O_{6.48}$*, Physical Review B **107** (10), 104508 (2023).

[2] A. Jiříčková, F. Antončík, M. Lojka, D. Sedmidubský and O. Jankovský, *Heat capacity and thermal stability of $YBa_2Cu_3O_7$*, AIP Conference Proceedings **1988** (1), 020018 (2018).

[3] A. Gupta, A. Kumari, S. K. Verma and B. D. Indu, *The phonon and electron heat capacities of cuprate superconductors*, Physica C: Superconductivity and its Applications **551**, 55-65 (2018).